

## RESEARCH ARTICLE

# $^{18}\text{F}$ -FDG uptake in denervated muscles of patients with peripheral nerve injury

Ji Soo Choi<sup>1</sup>, Han Gil Seo<sup>1</sup>, Byung-Mo Oh<sup>1</sup>, Hongyoon Choi<sup>2</sup>, Gi Jeong Cheon<sup>2</sup>, Shi-Uk Lee<sup>3</sup> & Seung Hak Lee<sup>4</sup> <sup>1</sup>Department of Rehabilitation Medicine, Seoul National University Hospital, Seoul, Republic of Korea<sup>2</sup>Department of Nuclear Medicine, Seoul National University Hospital, Seoul, Republic of Korea<sup>3</sup>Department of Rehabilitation Medicine, Seoul National University Boramae Medical Center, Seoul, Republic of Korea<sup>4</sup>Department of Rehabilitation Medicine, Asan Medical Center, College of Medicine, University of Ulsan, Seoul, Republic of Korea

## Correspondence

Seung Hak Lee, Department of Rehabilitation Medicine, Asan Medical Center, College of Medicine, University of Ulsan, 88, Olympic-ro 43-Gil, Songpa-Gu, Seoul 138-736, Korea.  
Tel: +82-2-3010-1694; Fax: Fax +82-2-3010-6964; E-mail: seunghak@gmail.com

## Funding information

This work was supported by a grant from the National Research Foundation of Korea (NRF), which is funded by the Korean government (Ministry of Science, ICT & Future Planning) (No.2015R1C1A1A02037192).

Received: 26 May 2019; Revised: 8 August 2019; Accepted: 1 September 2019

*Annals of Clinical and Translational Neurology* 2019; 6(11): 2175–2185

doi: 10.1002/acn3.50899

## Abstract

**Objective:** We aimed to investigate the clinical significance of increased uptake in  $^{18}\text{F}$ -fluorodeoxyglucose positron emission tomography in patients with peripheral nerve lesions. **Methods:** We selected patients with unilateral peripheral nerve lesions confirmed with electromyography who had undergone  $^{18}\text{F}$ -fluorodeoxyglucose positron emission tomography covering the lesions. In the denervated muscles and their contralateral corresponding pairs, a mean (SUV-mean) and maximum standardized uptake value (SUVmax) were obtained from  $^{18}\text{F}$ -fluorodeoxyglucose positron emission tomography images. We analyzed the difference in these values between the denervated and normal muscles. The lesion-to-normal ratio of the SUVmean (LNRmean) between each muscle pair was also obtained. Subgroup analysis was performed to find whether these three parameters were related to severity, abundance of abnormal spontaneous activity, and etiology. **Results:** Twenty-three patients with 38 denervated muscles were included. Compared to their normal counterparts, the denervated muscles showed significantly higher SUVmax ( $1.33 \pm 0.49$  vs.  $1.10 \pm 0.37$ ,  $n = 38$ ,  $P < 0.001$ ) and SUVmean ( $0.91 \pm 0.31$  vs.  $0.77 \pm 0.28$ ,  $n = 38$ ,  $P < 0.001$ ). The muscles with severe neuropathy showed significantly higher LNRmean than those with mild neuropathy ( $1.30 \pm 0.36$ ,  $n = 19$  vs.  $1.11 \pm 0.24$ ,  $n = 19$ ;  $P = 0.046$ ), and the muscles with traumatic neuropathy showed significantly higher LNRmean than those with nontraumatic neuropathy ( $1.32 \pm 0.28$ ,  $n = 13$  vs.  $1.14 \pm 0.33$ ,  $n = 23$ ;  $P = 0.015$ ). **Interpretation:** Denervated muscles with peripheral nerve injury showed higher uptake than normal muscles in  $^{18}\text{F}$ -fluorodeoxyglucose positron emission tomography, and this was associated with severity and etiology.

## Introduction

Peripheral nerve injury is a common neuromuscular disorder manifesting as pain, numbness, or paralysis. It can be caused by trauma, including iatrogenic injury, and nontraumatic conditions such as compression, tumor, or other systemic diseases. Although localized neuropathy rarely causes mortality, it certainly affects the function in daily living.<sup>1</sup>

Clinicians can determine the location and severity of nerve injury using electrophysiological methods, such as nerve conduction studies (NCS) and needle

electromyography (EMG).<sup>2</sup> In denervated myocytes, resting membrane potential is increased to the threshold level of activation and lead to abnormal spontaneous activity (ASA).<sup>3</sup> It can be detected in the form of fibrillation potential or positive sharp waves, known as denervation potentials, in EMG.<sup>4</sup>

However, needle EMG has several disadvantages, notably invasiveness and pain.<sup>5</sup> Moreover, interpretation of the findings is rather subjective.<sup>6</sup> To avoid these problems, magnetic resonance imaging and ultrasonography have been used to assess nerve damage.<sup>7–9</sup> However, these radiological examinations rely largely on nonspecific

morphological changes, such as edema and fibrotic changes.<sup>10,11</sup> Recently, magnetic resonance neurography has been used to visually demonstrate peripheral nerve pathologies more precisely, but most imaging techniques still remain complementary.<sup>12–14</sup> Therefore, we designed a functional imaging study to characterize the electrophysiological change after nerve injury.

Behera et al reported that denervated muscles showed increased uptake in <sup>18</sup>F-fluorodeoxyglucose (FDG) positron emission tomography (PET) in an animal model.<sup>15</sup> We clarified this phenomenon in a controlled animal study.<sup>16</sup> Our recent study investigated its mechanisms and temporal characteristics to explore its potential as a diagnostic tool for peripheral nerve injury.<sup>17</sup> We also reported a human case series of patients with iatrogenic spinal accessory neuropathy who showed increased uptake in the trapezius muscles in FDG-PET.<sup>18</sup>

FDG-PET is widely used to assess musculoskeletal tumors.<sup>19,20</sup> However, since physiological muscle contraction can become a source of false-positives,<sup>21</sup> the uptake signal of muscle is often ignored during interpretation. Since previous findings have implied that glucose hypermetabolism is a universal phenomenon in denervated muscles, it must be confirmed in clinical settings and explored as the basis for a new diagnostic method.

In this study, we ascertained whether denervated muscles showed higher FDG-PET uptake than normal muscles in patients with peripheral nerve lesion, and whether the increased uptake was correlated with clinical parameters.

## Subjects and Methods

### Patients

We reviewed the medical records of our EMG clinic to extract records of patients who had undergone both EMG and PET between 2010 and 2014. The inclusion criteria were (1) age over 18 years at the time of EMG and PET, (2) localized peripheral nerve lesion with denervation potentials, and (3) FDG-PET taken after neurological symptom onset and covering denervated muscles. The exclusion criteria were (1) EMG of the facial, laryngeal, or tongue muscles only, (2) diagnoses other than localized peripheral nerve lesion, (3) bilateral neuropathy involving the same myotome on each side, and (4) PET that did not cover the denervated muscles. In each patient, the EMG-confirmed denervated muscles were identified on the FDG-PET image. According to these criteria, 498 patients were screened; 23 patients with 38 denervated muscles were included (Fig. 1). This study was approved by the Institutional Review Board of our hospital, and the requirement for informed consent was waived because of its retrospective nature.

### Electrophysiological Study

In all studies, Medelec Synergy Plinth (Oxford Instruments, UK) or Nicolet EDX (Natus Neurology Inc., USA) portable electrodiagnostic systems was used. In the NCS, onset latency and amplitude of compound muscle action potential (CMAP), and sensory nerve action potential, were measured in the peripheral nerves of the upper or lower limbs.

In EMG, a monopolar electrode (Disposable Monopolar Needles; Natus Neurology, USA) was used. If ASA was detected in two of four needle sampling directions, it was graded as 1+. If it was detected in three of four sampling directions, it was graded as 2+. If ASA was detected in all sampling directions, it was graded as 3+. If the EMG baseline was obliterated by ASA at all sites, it was graded as 4+.<sup>4,22</sup> The morphology, recruitment, and interference patterns of motor unit action potentials (MUAPs) were evaluated from volitional muscle activity. The electrophysiological diagnosis was based on the distribution of neurological abnormalities, considering the NCS and EMG results. The severity of neuropathy was graded as either mild or severe based on electrophysiological findings. Specifically, injury of a nerve innervating the muscle was graded as “severe” only if CMAP were undetectable, or only if none or single MUAP was observed during maximal volitional activity. All electrophysiological studies were performed and interpreted by experienced electromyographers.

### FDG-PET

In 22 patients, FDG-PET images were acquired using dedicated PET/CT scanners (Biograph True point 40 with V and Biograph mCT 40; Siemens, Germany), combining a full-ring PET scanner with 2 mm resolution and a 40-slice spiral CT scanner. In one patient, a PET/MR scanner was used (Biograph mMR, Siemens, Germany), combining a full-ring PET with a 3.0-T MR scanner. Before FDG-PET, patients were required to fast for at least 8 h, avoid exercise, and discontinue drugs that can affect the result. Patients' blood sugar was tested before FDG injection, and the study was rescheduled if the level was higher than 11.1 mmol/L. An FDG dose of 5.18 MBq/kg was intravenously administered. Sixty minutes after FDG injection, emission scans were acquired while the patients lay supine in the scanner. The routine protocol covered the region from the base of the skull to the upper thighs; the lower legs were selectively covered in indicated patients. An FDG-PET examination time of 2 min per bed position, with 5–7 bed positions, was used. The acquired images were reconstructed using iterative ordered-subset expectation maximization True-X

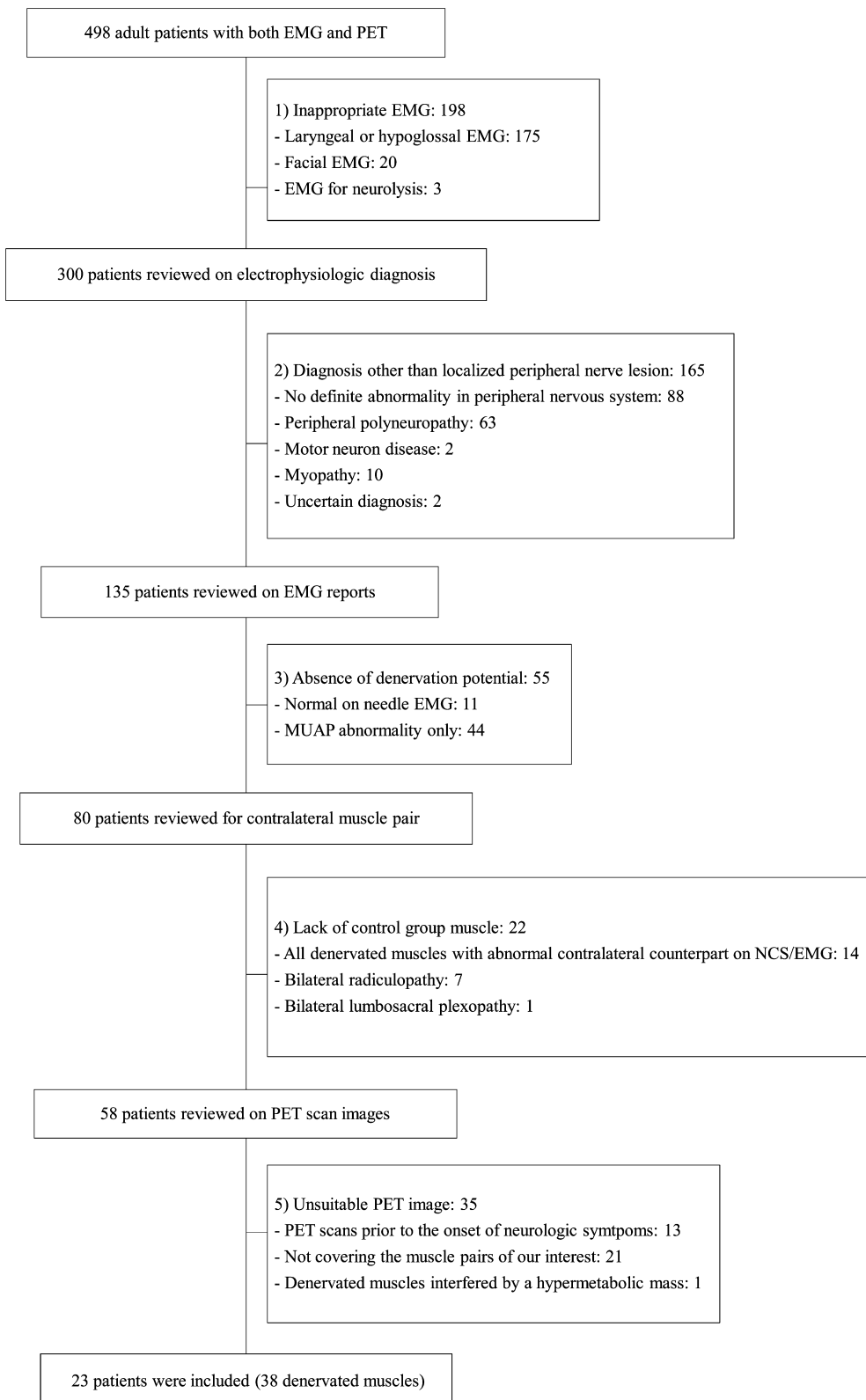
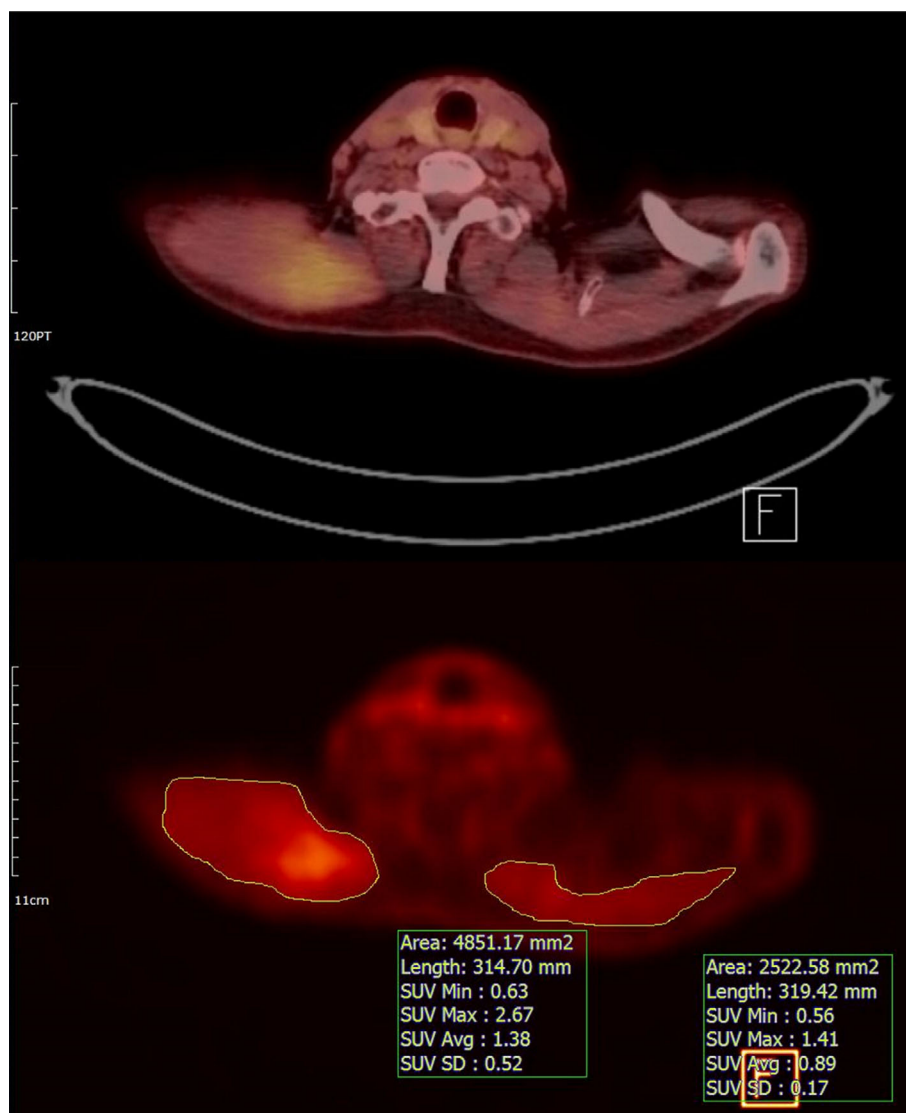


Figure 1. Flowchart of retrospective study design.



**Figure 2.** Illustrative case of a patient with right spinal accessory neuropathy. The trapezius muscles were identified bilaterally in the PET-CT fusion image (top), and ROIs were encircled on the PET image (bottom) at the most hypermetabolic sections of the trapezius muscles.

algorithms. The size of the reconstructed voxel was 3.12 mm × 3.12 mm × 4.98 mm.

### Comparison with a standardized uptake value

On the PET images of each patient, we localized the muscles that showed denervation potentials upon EMG. The axial cut containing the most hypermetabolic area of the muscle was determined by visual assessment, and this region of interest (ROI) was manually drawn along the circumference of the muscle in that image (Fig. 2). In each ROI, the standardized uptake value (SUV) was

provided as both a maximal and average value. The axial images of the slices just superior and inferior to the most hypermetabolic area were subjected to the same process, for a total of three ROIs in each denervated muscle. Among the maximal SUVs of the three ROIs in each muscle, the highest value was defined as the maximal uptake value (SUVmax) of the muscle. The mean SUV of the three ROIs in each muscle was defined as the mean uptake value (SUVmean) of the muscle.

For each denervated muscle, the anatomically corresponding muscle on the contralateral side was selected as a control. The SUVmax and SUVmean of each control were also obtained. The SUVmax and SUVmean of the

**Table 1.** Clinical data of included patients.

No.	Sex	Age	Chief complaint	Onset of EMG (weeks)	EMG to PET <sup>1</sup> (weeks)	Nerve lesion	Severity	Etiology <sup>2</sup>	Specific cause	Analyzed muscles
1	M	84	Arm weakness	12	18	Brachial plexopathy	Severe	Non-traumatic	Viral infection	D, IST, LS
2	F	66	Leg weakness	4	0	L3 radiculopathy	Mild	Non-traumatic	Collapsed L4 vertebra	IP, AL, RF, L3, L5 PSP
3	F	69	Arm weakness	4	-5	Brachial plexopathy	Mild	Non-traumatic	Tumor, 1 <sup>st</sup> rib	D, SST
4	F	59	Buttock tingling	5	19	S1-S4 radiculopathy	Severe	Traumatic	latrogenic	BF
5	M	66	Shoulder weakness	45	22	CN XI neuropathy	Severe	Traumatic	latrogenic	TPZ
6	F	50	Leg weakness	17	85	CN XI neuropathy	Mild	Traumatic	latrogenic	TPZ
7	M	64	Leg weakness Arm weakness	18	-9	Lumbosacral plexopathy C6 radiculopathy	Severe Mild	Traumatic	Fall down	BF D, BB, TB
8	F	48	Leg weakness	52	-6	Lumbosacral plexopathy	Mild	Undetermined	Not definite	Gmed
9	F	54	Leg weakness	52	-10	Lumbosacral plexopathy	Severe	Non-traumatic	Radiotherapy	Gmed, BF
10	M	65	Shoulder weakness	18	36	CN XI neuropathy	Mild	Traumatic	latrogenic	TPZ
11	M	53	Arm weakness	67	3	Brachial plexopathy,	Severe	Traumatic	latrogenic	BB
12	F	41	Foot drop	104	1	Sacral plexopathy	Severe	Non-traumatic	Tumor, sciatic foramen	BF
13	F	56	Thigh pain	12	1	Obturator neuropathy	Severe	undetermined	Not definite	AL
14	F	56	Leg weakness	2	43	Obturator neuropathy	Severe	Traumatic	latrogenic	AL
15	F	53	Arm weakness	16	-15	Brachial plexopathy	Mild	Non-traumatic	Tumor, shoulder	D, IST, BB
16	F	35	Leg weakness	104	-1	Sacral plexopathy L5 radiculopathy	Severe Mild	Non-traumatic	Tumor, sacrum	GCM
17	M	76	Leg numbness	2	5	L5 radiculopathy	Severe	Non-traumatic	L4/5 HIVD	L5
18	F	80	Hand pain	8	-1	C7 radiculopathy	Mild	Non-traumatic	Tumor, C6-T1 vertebrae	ECRL
19	F	61	Shoulder weakness	52	0	CN XI neuropathy	Severe	Non-traumatic	Tumor, salivary gland	TPZ
20	M	58	Leg weakness	40	1	Lumbosacral plexopathy	Severe	Non-traumatic	Tumor, presacral	Gmed
21	F	22	Leg weakness	28	-7	Lumbar plexopathy	Severe	Non-traumatic	Tumor, iliopsoas	VM
22	F	54	Leg numbness	8	99	CN XI neuropathy	Severe	Traumatic	latrogenic	AL, AM
23	M	58	Shoulder weakness	6	20	CN XI neuropathy	Mild	Traumatic	latrogenic	TPZ

CN XI, cranial nerve XI; HIVD, herniated intervertebral disc; D, deltoid; IST, infraspinatus; IP, iliopsoas; AL, adductor longus; RF, rectus femoris; PSP, paraspinatus; SST, supraspinatus; BF, biceps femoris; TPZ, trapezius; BB, biceps brachii; TB, triceps brachii; Gmed, gluteus medius; GCM, gastrocnemius (medial head); PL, peroneus longus; ECRL, extensor carpi radialis longus; AM, adductor magnus.

<sup>1</sup>Time interval from EMG to PET is provided, and negative values indicate that PET was performed prior to EMG.

<sup>2</sup>Nontraumatic etiology includes entrapment neuropathy, radiculopathy with herniated intervertebral discs, tumor invasion, herpes zoster infection, and radiotherapy-induced neuropathy.

denervated and the control muscles were collected to confirm the hypothesis: denervated muscles show higher SUV than control muscles. We also obtained the lesion-to-normal ratio of the SUVmean (LNRmean) between the denervated muscles and their contralateral controls.

### Subgroup analysis

Patients were classified into subgroups according to neuropathy severity, ASA abundance, and neuropathy etiology. Neuropathy severity was recorded as either severe or mild. ASA abundance was graded from 1+ to 4+ based on EMG findings. We categorized the etiology of neuropathy in each patient into one of three groups: traumatic, nontraumatic, or undetermined. Traumatic etiology included definite traumatic events involving peripheral nerve lesions. Nontraumatic etiology included

entrapment neuropathy, herniated intervertebral discs, tumor invasion, viral infection, and radiotherapy-induced neuropathy. If we could not determine whether the nerve lesion was caused by trauma, it was classified as having undetermined etiology. For each parameter, subgroup analyses of the SUVmax, SUVmean, and LNRmean were performed to determine statistical differences. Furthermore, the time interval between the onset of neurological symptoms and the date of PET was calculated when available, to plot PET uptake variables against time to elucidate their relationship.

### Statistical analysis

The datasets of the denervated and control groups were checked using Shapiro–Wilk analysis. It showed nonnormal distribution, so the SUVmax and SUVmean were

**Table 2.** Indication for <sup>18</sup>F-fluorodeoxyglucose positron emission tomography in the included patients and related clinical information.

No.	Primary cancer	RT field	Postoperative time at FDG-PET (months)	Post-RT time at FDG-PET (months)	Indication for FDG-PET
1	Follicular lymphoma(Rt. inguinal node)	N/A	N/A	N/A	suspected recurrence
2	Lung cancer	L4	44	17	suspected recurrence
3	Breast cancer, Lt.	C1-T1	175	64	response evaluation
4	Cervical cancer	N/A	6	N/A	suspected recurrence
5	Glottic cancer	Neck	16	13	surveillance
6	Thyroid cancer	N/A	24	N/A	surveillance
7	Kidney cancer, Lt.	N/A	38	N/A	suspected recurrence
8	Rectal cancer	N/A	27	N/A	response evaluation
9	Cervical cancer	Pelvis	69	128	suspected recurrence
10	Olfactory neuroblastoma	Head	13	11	surveillance
11	Thyroid cancer	N/A	16	N/A	surveillance
12	Cervical cancer	Pelvis	23	18	suspected recurrence
13	Urethral cancer	N/A	6	N/A	suspected recurrence
14	Ovarian cancer	N/A	22	N/A	suspected recurrence
15	Multiple myeloma(Spine, ilium)	N/A	N/A	N/A	suspected recurrence
16	Osteosarcoma(Rt. Sacrum)	Sacrum	8	6	suspected recurrence
17	Gastric cancer	N/A	29	N/A	suspected recurrence
18	None	N/A	N/A	N/A	diagnosis of malignancy(C6-T1 vertebrae)
19	None	N/A	N/A	N/A	diagnosis of malignancy (submandibular gland)
20	Rectal cancer	Pelvis	54	54	suspected recurrence
21	Nerve sheath tumor(Rt. femoral nerve)	N/A	1	N/A	RT planning
22	Endometrial cancer	N/A	25	N/A	surveillance
23	Salivary duct cancer	Head	6	3	response evaluation

RT, radiation therapy; N/A, not applicable.

compared using Wilcoxon signed-rank test. Between subgroups, the SUVmax, SUVmean, and LNRmean were compared using either the Mann–Whitney or Kruskal–Wallis test. Spearman's correlation analysis was performed to find the relationship between ASA abundance and PET parameters (SUVmax, SUVmean, and LNRmean), and between the time interval from the onset of symptoms to PET and the PET parameters. Statistical significance was defined as a *P*-value < 0.05.

## Results

### Patient characteristics

Totally, 23 patients were analyzed, with 38 muscles that showed ASA in EMG and were covered by PET. Clinical data of the included patients are summarized in Table 1 and 2. All patients with traumatic injury had partial axonotmesis; none had complete axonotmesis. The mean time interval from EMG to PET was  $13 \pm 29$  weeks. The time interval from the onset of neurological symptoms to the date of PET was more than 1 month in all but one patient, and more than 6 months in 14 patients. The exact date of neuropathy onset was identified in nine patients, all of whom had traumatic etiology. All but two

patients had been diagnosed with cancer before they underwent PET; two patients were diagnosed with cancer by the PET (Table 2).

### FDG-PET signal in denervated muscles

In 38 denervated muscles, the SUVmax was  $1.33 \pm 0.49$  (median: 1.24), while it was  $1.10 \pm 0.37$  (median: 1.07) in control muscles. A Wilcoxon signed-rank test showed significant differences between the two groups. ( $Z = 3.599$ ,  $P < 0.001$ ). The SUVmean of the denervated muscles was  $0.91 \pm 0.31$  (median: 0.88), which was higher than that of the control ( $0.77 \pm 0.28$ ; median: 0.69) with statistical significance ( $Z = 3.857$ ,  $P < 0.001$ ; Fig. 3). The LNRmean of all 38 muscle pairs was  $1.20 \pm 0.31$ .

### Subgroup analysis

Neuropathy was severe in 15 patients with 19 denervated muscles and mild in 10 patients with 19 denervated muscles (Table 1). Two patients had concurrent anatomical lesions of varying severity. The LNRmean of the severe subgroup was  $1.30 \pm 0.36$  (median: 1.18) while that of the mild subgroup was  $1.11 \pm 0.24$  (median: 1.07), which

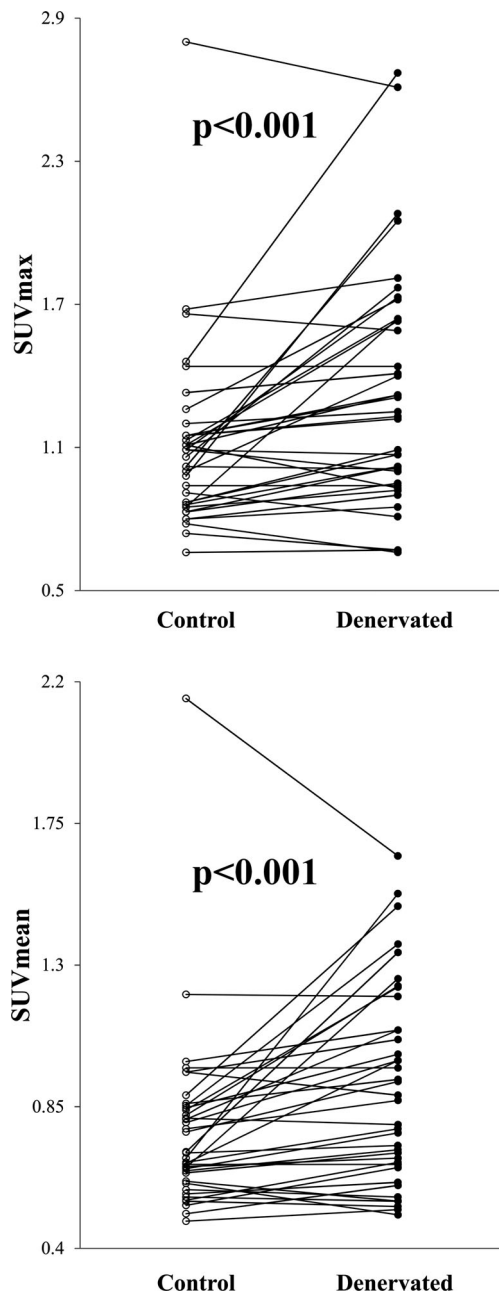


**Figure 3.** Scatter plots of SUVmax (top) and SUVmean (bottom) of the denervated and control muscles. The denervated muscles showed significantly higher SUVmax and SUVmean than the control muscle (SUVmax:  $1.33 \pm 0.49$  vs.  $1.10 \pm 0.37$ ,  $P < 0.001$ ; SUVmean:  $0.91 \pm 0.31$  vs.  $0.77 \pm 0.28$ ,  $P < 0.001$ ).

was significantly lower (Mann–Whitney test:  $U = 112.5$ ,  $P = 0.047$ ). The SUVmax and SUVmean showed no significant differences between the mild and severe subgroups ( $U = 176.5$ ,  $P = 0.914$  for SUVmax;  $U = 177$ ,  $P = 0.925$  for SUVmean; Fig. 4A).

The ASAs were graded as 1+, 2+, 3+, and 4+ in 6, 15, 15, and 2 muscles, respectively. The Kruskal–Wallis test failed to show significant difference among these four subgroups in SUVmax, SUVmean, and LNRmean ( $H = 1.043$ ,  $P = 0.791$  for SUVmax;  $H = 2.705$ ,  $P = 0.439$  for SUVmean;  $H = 1.873$ ,  $P = 0.599$  for LNRmean; Fig. 4B). Spearman correlation analysis showed no significant relationship between ASA and the three variables ( $r_s = 0.021$ ,  $P = 0.899$  for SUVmax;  $r_s = 0.101$ ,  $P = 0.548$  for SUVmean;  $r_s = 0.114$ ,  $P = 0.496$  for LNRmean).

The etiology of neuropathy was traumatic in nine patients with 13 denervated muscles, nontraumatic in 12 patients with 23 denervated muscles, and undetermined in two patients with two denervated muscles (Table 1). The LNRmean of traumatic and nontraumatic neuropathies were  $1.32 \pm 0.28$  (median: 1.22) and  $1.14 \pm 0.33$  (median: 1.07), respectively, and the difference was significant (Mann–Whitney test:  $U = 76$ ,  $P = 0.015$ ). No significant difference was found in SUVmax ( $U = 96.5$ ,  $P = 0.082$ ) or SUVmean ( $U = 117.5$ ,  $P = 0.300$ ) between the two subgroups (Fig. 4C).

The definite onset of neurological symptom was recorded in nine patients with 13 denervated muscles, all of whom had traumatic etiology. We plotted the SUVmax, SUVmean, and LNRmean against the time interval between onset of injury and date of PET (Fig. 5), but there was no demonstrable correlation ( $r_s = -0.393$ ,  $P = 0.184$  for SUVmax;  $r_s = -0.243$ ,  $P = 0.424$  for SUVmean;  $r_s = -0.114$ ,  $P = 0.710$  for LNRmean).

## Discussion

In this retrospective study, we used FDG-PET to show that denervated muscles have higher glucose metabolism than do normal muscles. Glucose metabolism showed significant difference, especially in patients with traumatic or severe nerve injury. These findings are in line with those in previous studies, although LNRmean values in this study were smaller than those in former reports. In rat models of complete sciatic nerve injury, the denervated muscles showed about 5 to 10-times higher uptake than contralateral muscles in FDG-PET.<sup>16,17,23</sup> In a human case series of patients with spinal accessory neuropathy, their denervated trapezius muscles showed about 2 to 3-times higher mean uptake than the unaffected side in FDG-PET.<sup>18</sup> However, the present study only showed an approximately 20% difference between the denervated and normal muscles in SUVs, perhaps because of heterogeneity between the studies. In the rat model, the duration and severity of nerve injury were significantly associated with LNRmean.<sup>17</sup> The human case series investigated patients with iatrogenic accessory neuropathy who

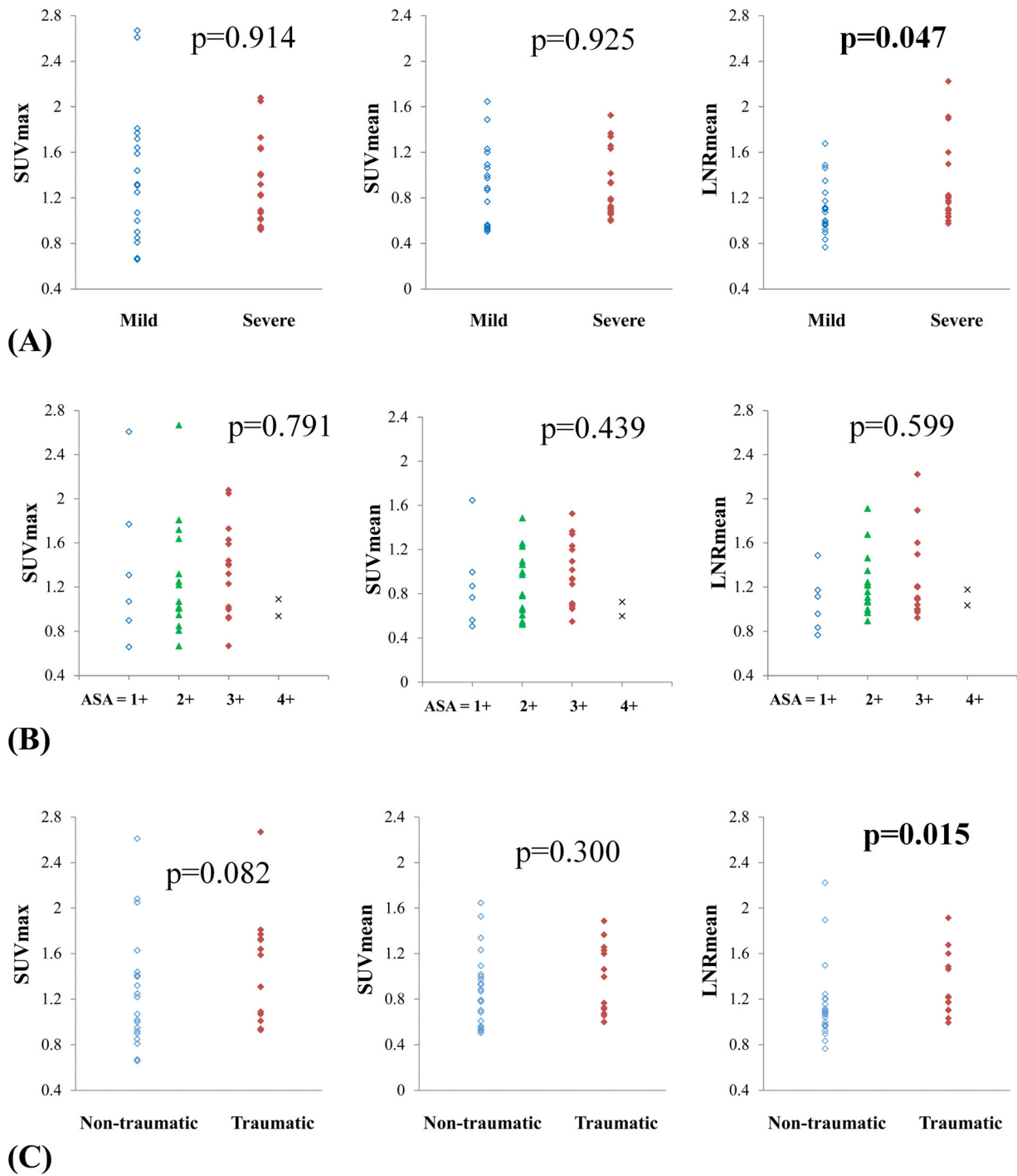


**Figure 4.** Scatter plots of SUVmax (left), SUVmean (middle), and LNRmean (right) in (A) mild and severe subgroups, (B) ASA grade 1 + to 4 + subgroups, and (C) non-traumatic and traumatic etiology subgroups. The LNRmean of the severe subgroup was significantly higher than that of the mild subgroup ( $1.30 \pm 0.36$  vs.  $1.11 \pm 0.24$ ,  $P = 0.047$ ), and the LNRmean of the traumatic subgroup was significantly higher than that of the nontraumatic subgroup ( $1.32 \pm 0.28$  vs.  $1.14 \pm 0.33$ ,  $P = 0.015$ ).

underwent PET less than 9 months after surgery.<sup>18</sup> In the present study, the severity and etiology of nerve injury, as well as the timing of FDG-PET, varied widely among

patients. Therefore, patients with mild, nontraumatic, or chronic-onset nerve lesions might have skewed the effect size.

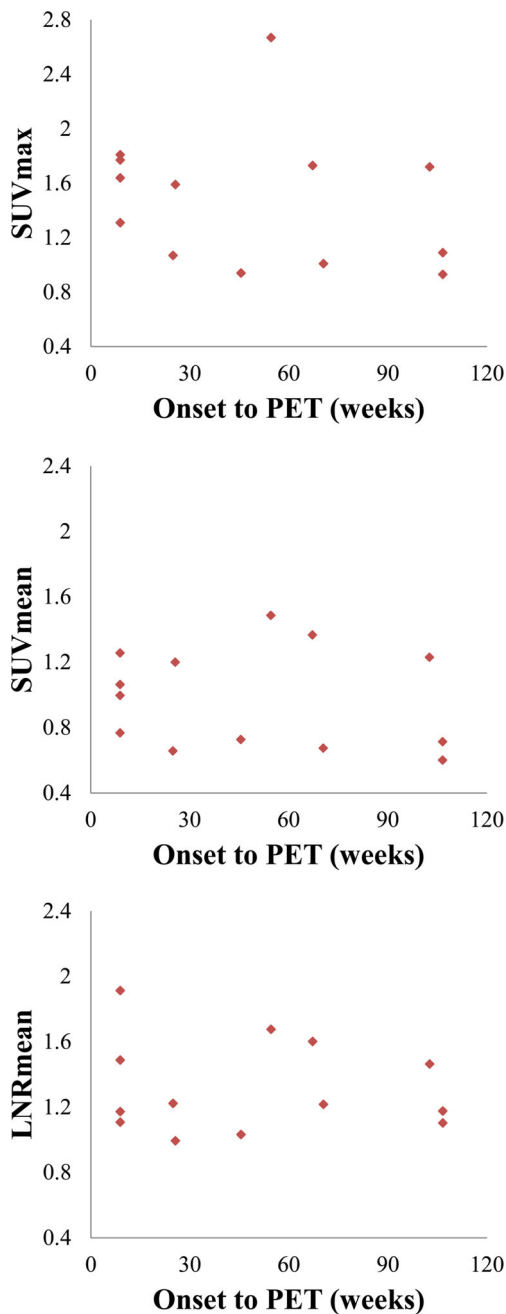


**Figure 5.** The SUVmax (top), SUVmean (middle), and LNR (bottom) of traumatic neuropathy are plotted against time interval between onset of symptoms and date of FDG-PET. No correlation was found between FDG-PET parameters and time interval.

In subgroup analysis, neuropathy severity affected the SUVs in denervated muscle. The neuropathy severity was determined based on both the CMAP amplitude and the MUAP activation patterns, which reflect the viability of axons.<sup>22</sup> However, it is difficult to quantify severity accurately, because CMAP amplitude is not obtainable in all

muscles, and the MUAP interpretation depends on the examiner's experience and patient's cooperation. In addition, it is technically difficult to evaluate the nerve injury severity in all muscular branches. In contrast, PET quantifies glucose metabolism in individual muscles using continuous variables. Therefore, it is interesting that we found a significant relationship between electrophysiologically graded severity and PET uptake values, considering the different characteristics of these two methodologies.

In contrast to severity, the ASA abundance was not significantly correlated with LNRmean (Fig. 4B). It takes several days for ASA to appear in the affected muscles, and it often disappears after several weeks<sup>3,24</sup> ASA is detectable using concentric or monopolar needle electrodes, which have a small recording area of 0.08 mm<sup>2</sup> and 0.17 mm<sup>2</sup>, respectively.<sup>4</sup> An electromyographer grades the abundance of ASA based on its appearance during multidirectional needling. Since ASA grading depends on these temporal, spatial, and examiner-dependent factors, it can be difficult to find a direct correlation with PET uptake values, unless such factors are well-controlled.

Traumatic etiology affected LNRmean in the present study. However it should be noted that the temporal course of nontraumatic neuropathy differs from that of traumatic injury. The patients with nontraumatic neuropathy in this study mostly had insidious-onset symptoms rather than acute damage. In cases of tumor infiltration or radiation therapy-induced neuropathy, neural damage progresses slowly.<sup>25,26</sup> Thus, the denervation-induced molecular changes may also be prolonged, taking a course different from that in traumatic neuropathies. However, due to the retrospective nature and small sample size of this study, we cannot differentiate the effect of trauma from that of time. Further prospective, controlled study is required to evaluate the effect of time on glucose uptake.

The present study had several limitations. Firstly, the time interval between EMG and PET, and that between nerve injury and PET, varied among the patients. Therefore, electrophysiological data may not reflect the actual state at the time of PET. Moreover, the postinjury time was heterogeneous and ranged from one week to two years. The underlying mechanisms of increased FDG uptake between patients who underwent FDG-PET one week and two years after injury might be different. Because a temporal course of glucose hypermetabolism in humans has not been reported yet, we aimed to assess the longitudinal temporal characteristics of this phenomenon by including patients across various postinjury time periods. However, a prospective study with controlled postinjury time is necessary for further investigation. Secondly, the muscles checked in the motor NCS were distal limb muscles, which were mostly not covered in the routine FDG-PET protocol. To more accurately establish the

relationship between severity and SUVs, denervated muscles with CMAP recordings should be covered in PET. Thirdly, FDG-PET can lead to false positivity because of several factors. Physiological glucose uptake during normal muscle contraction is one such factor.<sup>21</sup> If the patients failed to fully rest before PET, their control muscles may have shown significant glucose uptake. In denervated muscles, surgery or radiotherapy could alter the FDG uptake.<sup>27</sup> However, the sites of the surgical procedures and radiation were distant from the denervated muscles in our patients. Therefore, direct effect of surgery or radiation is less likely to be the source of increased FDG uptake. Fourthly, the process of SUV measurement is a potential source of error because of the subjective manual delineation of the ROIs. In some images, the muscle boundaries were not clear so the delineated ROIs may have included adjacent muscles. Identification of the spatial pattern of denervated muscles is essential to localize a nerve lesion.<sup>9,14</sup> Therefore, error in ROI delineation are crucial problem to be solved to establish PET as a new diagnostic modality for nerve injury. Solutions to this problem could be a prospective study with predetermined optimal voxel size and the use of standardized image software, which were not available in this retrospective study. In addition, relatively small sample sizes and effect sizes were another limitation. Moreover, it should be noted that the present study followed an unblinded approach, which did not permit the deduction of any inferences on the diagnostic value or performance of FDG-PET to identify cases of denervated muscles in patients with peripheral nerve lesions.

This study revealed that denervated muscles in peripheral nerve lesions showed higher SUVs than healthy muscles in FDG-PET, and it was associated with severity and etiology of nerve injury. The ultimate goal of our study is to use FDG-PET as a novel diagnostic tool for patients with peripheral nerve injury, but there are still many limitations. Further prospective controlled studies, particularly at the acute stage of denervation, are needed to establish the value of FDG-PET as new diagnostic tool for peripheral nerve lesions.

## Acknowledgments

This work was supported by a grant from the National Research Foundation of Korea (NRF), which is funded by the Korean government (Ministry of Science, ICT & Future Planning) (No.2015R1C1A1A02037192).

## Author Contribution

S.H.L., B.M.O., H.C., and S.U.L. created the concept, designed, and supervised the study. J.S.C., S.H.L., H.G.S., B.M.O., H.C., G.J.C., and S.U.L. analyzed and interpreted

data. J.S.C. and S.H.L. conducted experiments and drafted the manuscript. All authors read and approved the final version of the manuscript.

## Conflicts of Interest

Nothing to report.

## References

1. Cifu DX. Braddom's Physical Medicine and Rehabilitation 5th edition. 5th ed. Philadelphia: Elsevier Health Sciences, 2015.
2. Preston DC, Shapiro BE. Electromyography and neuromuscular disorders: clinical-electrophysiologic correlations. New York: Elsevier Health Sciences, 2012.
3. Thesleff S, Ward M. Studies on the mechanism of fibrillation potentials in denervated muscle. *The Journal of physiology* 1975;244:313–323.
4. Daube JR, Rubin DI. Needle electromyography. *Muscle Nerve* 2009;39:244–270.
5. Moon YE, Kim SH, Choi WH. Comparison of the effects of vapocoolant spray and topical anesthetic cream on pain during needle electromyography in the medial gastrocnemius. *Arch Phys Med Rehabil* 2013;94:919–924.
6. Kendall R, Werner RA. Interrater reliability of the needle examination in lumbosacral radiculopathy. *Muscle Nerve* 2006;34:238–241.
7. Wessig C, Koltzenburg M, Reiners K, et al. Muscle magnetic resonance imaging of denervation and reinnervation: correlation with electrophysiology and histology. *Exp Neurol* 2004;185:254–261.
8. Simon NG, Ralph JW, Lomen-Hoerth C, et al. Quantitative ultrasound of denervated hand muscles. *Muscle Nerve* 2015;52:221–230.
9. Kim SJ, Hong SH, Jun WS, et al. MR imaging mapping of skeletal muscle denervation in entrapment and compressive neuropathies. *Radiographics* 2011;31:319–332.
10. Zaidman CM, Seelig MJ, Baker JC, et al. Detection of peripheral nerve pathology: comparison of ultrasound and MRI. *Neurology* 2013;80:1634–1640.
11. Pillen S, Tak RO, Zwarts MJ, et al. Skeletal muscle ultrasound: correlation between fibrous tissue and echo intensity. *Ultrasound Med Biol* 2009;35:443–446.
12. Martin Noguero T, Barousse R, Socolovsky M, Luna A. Quantitative magnetic resonance (MR) neurography for evaluation of peripheral nerves and plexus injuries. *Quant Imaging Med Surg* 2017;7:398–421.
13. Chhabra A, Madhuranthakam AJ, Andreisek G. Magnetic resonance neurography: current perspectives and literature review. *Eur Radiol* 2018;28:698–707.
14. Schwarz D, Weiler M, Pham M, et al. Diagnostic signs of motor neuropathy in MR neurography: nerve lesions and muscle denervation. *Eur Radiol* 2015;25:1497–1503.

15. Behera D, Jacobs KE, Behera S, et al. 18F-FDG PET/MRI can be used to identify injured peripheral nerves in a model of neuropathic pain. *J Nucl Med* 2011;52:1308.
16. Lee SH, Oh B-M, Lee G, et al. Feasibility of 18F-FDG PET as a noninvasive diagnostic tool of muscle denervation: a preliminary study. *J Nucl Med* 2014;55:1737–1740.
17. Lee SH, Seo HG, Oh B-M, et al. 18F-FDG positron emission tomography as a novel diagnostic tool for peripheral nerve injury. *J Neurosci Methods* 2019;317:11–19.
18. Lee SH, Seo HG, Oh B-M, et al. Increased 18F-FDG uptake in the trapezius muscle in patients with spinal accessory neuropathy. *J Neurol Sci* 2016;362:127–30.
19. Aoki J, Endo K, Watanabe H, et al. FDG-PET for evaluating musculoskeletal tumors: a review. *J Orthop Sci* 2003;8:435–441.
20. Fletcher JW, Djulbegovic B, Soares HP, et al. Recommendations on the use of 18F-FDG PET in oncology. *J Nucl Med* 2008;49:480–508.
21. Yeung HW, Grewal RK, Gonen M, et al. Patterns of (18) F-FDG uptake in adipose tissue and muscle: a potential source of false-positives for PET. *J Nucl Med* 2003;44:1789–96.
22. Amato AA, Dumitru D. *Electrodiagnostic medicine*. 2002.
23. Pak K, Shin MJ, Hwang S-J, et al. Longitudinal changes in glucose metabolism of denervated muscle after complete peripheral nerve injury. *Mol Imag Biol* 2016;18:741–747.
24. Dorfman LJ. Quantitative clinical electrophysiology in the evaluation of nerve injury and regeneration. *Muscle Nerve* 1990;13:822–828.
25. Corbo M, Balmaceda C, Balmaceda C. Peripheral neuropathy in cancer patients. *Cancer Invest* 2001;19:369–382.
26. Delanian S, Lefaix J-L, Pradat P-F. Radiation-induced neuropathy in cancer survivors. *Radiother Oncol* 2012;105:273–282.
27. Bhargava P, Zhuang H, Kumar R, et al. Iatrogenic artifacts on whole-body F-18 FDG PET Imaging. *Clin Nucl Med* 2004;29:429–439.